Strains Induced in Urban Structures by Ultra-high Frequency Blasting Rock Motions; a Case Study

C. H. Dowding

Professor, Northwestern University, Department of Civil and Environmental Engineering, Evanston, IL, 60208, USA

E. Hamdi

Associate Professor, Université de Tunis El Manar – Ecole Nationale d'Ingénieurs de Tunis. LR14ES03-Ingénierie Géotechnique. BP 37 Le Belvédère, 1002 Tunis,Tunisia.

C. T. Aimone-Martin

Aimone-Martin Assoc. Socorro, NM, USA

ABSTRACT:

This paper describes measurement and interpretation of strains induced in two, multiple story, older, urban structures by ultra-high frequency rock blast excitation from contiguous excavation. These strains are obtained from relative displacements found by integrating time correlated velocity time histories from multiple positions on the structures and foundation rock. Observations are based on ten instrumented positions on the structures and in the foundation rock during eight blast events, which provided over seventy time histories for analysis. The case study and measurements allowed the following conclusions: Despite particle velocities in the rock that greatly exceed regulatory limits, strains in external walls are similar to or lower than those necessary to crack masonry structures and weak wall covering materials. These strains are also lower than those sustained by single story residential structures when excited by low frequency motions with particle velocities below regulatory limits. Expected relative displacements calculated with pseudo velocity single degree of freedom response spectra of excitation motions measured in the rock are similar to those measured.

KEY WORDS: displacements, shear and tensile strains, close-in rock blasting, urban structures, ultra-high frequency excitation, pseudo velocity spectral analysis, peak particle velocity.

1 INTRODUCTION

The case study summarized by this paper provides the multiple position, time-correlated, velocity time histories needed to advance understanding of response of urban structures to ultra-high frequency excitation. Current regulations and understanding are based upon measurements of the response of residential, 1 to 2 story structures (Siskind, et al 1980, Dowding, 2000). Extension of these observations by response spectrum analysis to taller structures when excited by high frequency excitation needs to be validated (Abeel, 2012). This paper provides the beginning of such validation.

Most often standard earthquake engineering assumes that excitation wave lengths are long enough that buildings are excited homogenously and respond synchronously. In other words excitation motions along the base of the structure are the same and response at the top occurs synchronously. For close-in rock blasting this is not the case. With high excitation frequencies (> 100 Hz for rock to rock transmission) the amplitudes and phase are likely to change along the bottom of the structure. For instance, with a propagation velocity of 3000 m/s, 150 Hz frequency and a distance along the bottom of the structure of 60 m, the excitation pulse would have traveled (60/(3000/150)=) 3 wave lengths and might have attenuated significantly (Woods & Jadele, 1985). In addition the time of arrival would not be equal at the ends of the building if the blast were detonated at one end. The peak would arrive some 60/3000 = 20 milliseconds later the other end. If the building were 5 stories high and had a fundamental response period of 0.5 sec., its response at the other end would be $(0.020/0.5)2\pi$ or 0.080π out of phase from the end where the blast was initiated.

This study provides the additional multiple position, time-correlated information to more fully define the response of these larger, more massive urban structures. Current regulations often only require that the excitation motions be measured at one location. Building response is then most likely to be considered as synchronous and similar to that measured by the Siskind's et al. (1980) work with smaller, less massive structures. There is no requirement to measure building response, and as a result compliance measurements provide no new information about the nature of response of larger buildings to ultra-high frequency excitation.

Discussion of the use of strain-based methods of vibration control can provide regulatory guidance. Changes in regulations based upon strain measurements can reduce the confusion in specifications, help define the most appropriate locations of measurement of response, and provide more appropriate construction controls. These changes should help reduce costs of urban construction in rock founded cities around the world.

The paper is divided into two main sections: Site& Instrumentation and Response. Site and Instrumentation is divided into four sections: site and geology, transducers, blasting practice and vibratory environment. Response is divided into three sections: differential displacement, strains, comparison with controls.

2 SITE AND GEOLOGY PRESENTATION

This study was conducted in a dense urban location where blasting was required not just adjacent to buildings but contiguous to them as shown by the photograph in Figure 1. Blast excavation was carried out at the two sites simultaneously which led to instrumentation of the two buildings and allowed response from a blast at one site to be measured at both buildings as well as two locations on the same building. Contiguous blasting produced excitation ground motions that were unusually high in amplitude and with ultra-high dominant frequencies.

The buildings were constructed in 1890 and 1920, and are typical of structures built in this city at that time. They are 4- to 6-stories high, with load bearing walls constructed of unreinforced brick masonry, which are thought to be 2 to 3 wythe thick. Floors of these buildings were constructed with wood joists. Recently the ground floor of building 2 was reconstructed as reinforced concrete to support the weight of fire trucks. Both structures have basements, exterior walls of which are shown by the photographs of the excavations shown in Figure 2

The rock supporting these structures is a mica schist whose foliation dips into the excavation from beneath the structures. It is a dark-gray to silvery, rusty-weathering, generally coarse grained, foliated but poorly layered to massive gneiss or schistose gneiss, composed of quartz, oligoclase, microcline, biotite, and muscovite, and generally sillimanite and garnet (Panish, 1992). Vertical rock faces are supported by rock bolts that are 3m to 10m long.

3 TRANSDUCER DESCRIPTION AND INSTALLATION

Buildings and rock were instrumented with geophone transducers that meet International Society of Explosive Engineers (ISEE) standards. They measure velocity and have flat responses between 2 and 250 Hz. These transducers were monitored with digital seismographs with output digitized at 2048 samples per second (sps). Seismographs begin recording (6 seconds duration with 0.25 seconds of pre-trigger) when the particle velocity exceeds a threshold. The threshold had to be set variably because of the background noise produced by mechanical, rock excavation through back-hoe ramming. Seismographs were connected in series to provide a common time base that was accurate within one sample interval of 0.0005 sec. When the closest seismograph detects ground motion that exceeds the threshold value, it begins recording and triggers the other sensors.

3.1 *Building 1 transducers*

Two geophones were placed at each of the north and south corners of the west wall nearest the excavation as shown in Figure 2 (a-left). Two were bolted at the building street level (denoted in the following as B (bottom) sensors) and two to the top of the wall (denoted hereafter sensors A). Vertical distance between the sensors B and A differs at the south and north locations because of the differing building geometry. The lower (B) transducers are bolted on brackets which in turn are bolted into the mortar between bricks on the building about 1 m (3-4ft) above street level. The upper (A) transducers are also bolted to brackets and bolted into the mortar onto the inside of the parapet wall just above roof mastic.

Each geophone contained two transducers; one in the radial direction, parallel to the west wall and the other in the transverse direction, perpendicular to the west wall. All four transducers (two upper and two lower) at a corner were connected to one, four channel seismograph to provide a common time stamp. South and north seismographs were connected to provide a common time stamp.

In addition one triaxial geophone was installed in the rock beneath the north corner with the radial parallel and the transverse perpendicular to the west wall. These rock geophones were connected to the building seismographs to provide a common time stamp. Typical construction interference and back-hoe ramming reduced the number of blast events wherein rock measurements were possible during blast events. Also construction interaction prevented installation of rock transducers altogether at the south end

3.2 *Building 2 transducers*

Building 2 was instrumented in a manner similar to that of building 1 as shown in Figure 2 (b-right). As with building 1, geophones were placed at the lower (B) and upper (A) parts of the west wall with radial parallel and transverse perpendicular to the wall. North A transducers with bolted to the inside of the upper tower portion instead of the parapet location. As with Building 1, all four transducers (two upper and two lower) at a corner were connected to one, four channel seismograph to provide a common time stamp. South and north seismographs were connected to provide a common time stamp.

Two other transducers were also bolted to building 2. One transversely sensitive transducer was bolted to the inside of the basement wall at mid height, 10 m (33 ft) north of the south wall. A second, vertically sensitive transducer was mounted to the underside to the basement ceiling (first floor) also 10 m north of the south wall. They were also wired to

Additionally, one triaxial geophone was bolted to the vertical rock face beneath building 2 at the south end and time correlated with structure measurements. This geophone was also oriented with radial parallel and transverse perpendicular to the west wall. As shown in Figure 2, it was installed 0.9m below the basement floor level.

Time correlation connections and timing of transducer installation were difficult to coordinate with construction and blasting. As is true for instrumentation of any construction project, many opportunities are lost because of either timing or construction difficulties. There was no provision for time correlation between the two buildings, as the distance was too large and the cable route too complex. While much of the data obtained for bottom (B) and top (A) responses is time correlated, correlation between corners was difficult to obtain because of connection challenges. Because of late installation, rock response is missing for all but five of the blasts. Events reported herein are those where all motions of a building were time correlated.

4 BLASTING PRACTICE

Rock fragmentation and excavation was accomplished with close-in blasting techniques. Blasts are initiated by a Nonel initiation system. Holes are delayed with 25 and 17 ms surface delays with 500 ms in-hole delays. A blast typically contains 20-50 holes with 2 to 10 rows. The holes are arranged in a spacing and burden pattern of less than 60cm x 60cm (2ft x 2ft). There is usually at least one free vertical face, and often two. Blast holes are charged with a combination of two explosives types of emulsion explosive. Because of limitations of blast-induced vibration peak particle velocity, the number of holes per volume of fragmented rock is often high, hole diameter is small and in-hole delays are used. There were at total of 8 blasts designated a through h used in this study. Charge weights per delay varied from 2.41to 2.96 kg. Scaled distances and absolute distances from the north corner of Building 1 varied from 7.5 to 14.1 (m/kg^2) and 1.9 to 19.8 for events f and a respectively.

5 GROUND MOTION ENVIRONMENT

Ground motions monitored in this study produced peak particle velocities (PPV's) that attenuate at expected rates when plotted against square root scaled distance. Ground motion data from the rock below the structures were available for five of the blasts, four under building 1 and one under building 2. Figure 3 plots the values of peak velocity against scaled distance for these five blasts as well as expected values given by Oriard (1972). The lines on the plot are lower and upper bounds of expected values as well as upper bound of expected values for highly confined blasts. Four of the five plotted points from this study fall within the normal bounds of expected values, and all five fall below the upper bound for confined blasts. As these blasts are indeed confined, these data are in the expected range given by Oriard and are not unusual.

These rock to rock motions occur at unusually high frequencies (140 to 500 Hz) and produce unusually low building response as shown by the response spectra of the rock motions in Figure 4. Rock motions are rarely measured in urban blasting because the geometry of most immediately adjacent urban excavations only allows measurement at the street (B) level, because rock is inaccessible at the beginning and changes elevation with the adjacent excavation.

There are many possible explanations for the lower PPV's on the building at the street level. Large mismatches between response and excitation frequencies (0.5 and 500 Hz) results in very low velocity response as shown in the response spectrum in Figure 4. The small energy in a

500 Hz pulse is not sufficient to excite these relatively massive (compared to a one story suburban or rural residence) structures. The impulse is so small (due to its extremely small duration) that it imparts little change in the momentum of the structure. High attenuation and change in phase along the structure, creates high damping overall and low response.

5.1 *Integration of velocity time history*

As described in the introduction, strains associated with the fundamental, dominant, or first mode of response can be calculated from time correlated displacements, which were developed by integrating the velocity time histories. Before calculation of strains, the velocity time histories were corrected for baseline irregularities. An example of the four steps in this correction process is shown in Figure 5. First, the velocity time history (a) is baseline corrected. Linear and second order polynomial baseline corrections were tested as shown in (b). As can be seen the polynomial correction did not remove the low frequency (~ 2 Hz artifact) that is not in the original velocity time history. It was removed by subtracting the 200 point central-moving–average (continuous line) (c) to produce the displacement time history that oscillates about 0 as shown in (d).

5.2 *Differential displacement calculation*

Prior to the calculation of strains, the differential structure motions were computed from the difference between displacements at the upper, A, and lower, B, transducer positions as illustrated in Figure 6 for event 06/06. Velocity time histories are first integrated using the procedure described in the previous section to obtain displacement time histories. Then the differential displacement is found by simple subtraction of the two displacements (at A & B) at the same time. These differential displacements are then searched for the largest. Plots of the transverse velocities recorded at upper and lower transducers of Building 1, as well as corresponding displacements and differential displacements time histories for the06/06 event are shown in Figure 6.

Table A in the Appendix compares the maximum calculated differential displacements between measurement points and PPV's induced by all eight events. The maximum recorded whole or super-structure differential displacement was 334.4μm between the rock (G) and lower (B-street) levels at the north corner of building 1 during the 06/09 event. The maximum calculated differential displacement between bottom (B) and top (A) was 178.7 μm at the north corner of the building 1 during the 07/07 event.

Appendix B contains all velocity and displacement time histories for events 06/06 and 06/09.

6 STRAIN CALCULATIONS

6.1 *Procedure for calculating strains*

Two types of strain can be calculated: a) distortion parallel to the plane of the wall and b) distortion perpendicular to the plane of the wall (Dowding, 2000). First consider distortion parallel to the plane of a building wall, which produces shear strains that can be calculated as:

$$\gamma = \frac{\delta}{L} \qquad (1)$$

where L is the wall or building height and δ is the distortion or difference of displacement between the top and bottom of the wall in a direction parallel to the plane of the wall . This shear strain can be translated into tensile strains, ε_t, as follows:

$$\begin{gathered} \varepsilon_t = \frac{\delta}{L}\sin\varphi\cos\varphi\ ; \\ \varphi = \arctan(H/W) \end{gathered} \qquad (2)$$

where H is the wall height (or in this case the vertical distance between transducer location) and W is the width (not thickness) of the wall or building face on which the transducers are located. The H and W's employed in these calculations are visible in Figure 2 and are enumerated in a footnote in the Appendix A table.

Now consider distortion in a direction perpendicular to the plane of the wall, which produces bending strains in the wall. A beam deflection model with a measured relative displacement, δ, requires a deflection shape to calculate strains. The deflection shape is controlled by the end conditions of the beam, which can be fixed or free. A "fixed-fixed" end condition describes the most distorted shape consistent a single maximum δ, and was used to calculate the strain from the relative displacement, δ , between two transducers

$$\varepsilon = \frac{6\delta c}{L^2} \qquad (3)$$

where c is the distance from neutral axis to most extreme fiber, taken here as half the wall thickness and L is the length of the beam or in this case the height of the wall or distance between the two transducers, H. For calculations in this study, the walls were assumed to be

180 mm (7 in) thick. The fixed-fixed end condition describes the most distorted shape and thus the highest strain with a single relative displacement, δ, that is measured or estimated through single degree freedom response analysis. The other distortion shape consistent with a single δ, is "fixed-free", strains would be one-half that for "fixed-fixed". Fixed-fixed and fixed-free distortion shapes are illustrated in mechanics of materials and structural analysis text books and Dowding (2000).

6.2 *Induced Strains*

Appendix A enumerates and compares all the PPV's and maximum strains induced in the two buildings by the eight blast events. As described above these strains were calculated from the differential displacements that are also compared in this table. Maximum and minimum global (A-B) in-plane shear strains were 15.0 and 0.3μ-strains respectively. Corresponding maximum in-plane tensile strain calculated was 2.8μ-strains.

The blast induced strains are low despite high excitation particle velocities. They vary from blast to blast as would be expected. All of the strains are smaller to the south in building 1, which is some 60 m south of the blasts located at the north corner as shown in Figure 1. This consistently smaller differential displacement (A-B) results from the attenuation of the ground motions along the base of the structure. North to south declination on strain ranges from 75% to 97% for the radial strains and from 70% to 96% for the transverse strains.

Reduction of the number of examples in Appendix A to those in Table 1 with rock excitation motions more simply illustrates these observations and those to follow. Among other things it compares basement responses (columns 1-5) with those of the upper stories (columns 6-10). Basement response is complex. While in-plane shear and tensile strains in the basement can be calculated from the differential displacements there is no amplification or whole body synchronous response. There is no amplification because superstructure and component natural frequencies fall on the extreme displacement boundary of the response spectrum in Figure 4. The structures are too massive to respond. In addition the street level floor is not free to move laterally as is the building above because the basement walls supporting it are restrained from lateral movement by the soil and infrastructure surrounding the basement walls. This restraint further reduces the energy transmitted to the floors above as shown in the discussion below.

Comparison of basement and upper story strains show the degree to which the differential displacements decline in the above-ground section of the building. The ratio between the upper building shear strains (columns 6-10) and the basement shear strains (columns 1-5) ranged from 10% to 73% in the transverse direction. As discussed above this declination is expected as the lower portion of the building absorbs the vibratory energy first. The greatest declinations of strains above the basement level occurred with rock motions at the north end of building 1 that exceeded 75 mm/s (3 ips). The largest excitation motion was some 200 mm/s (8 ips). These high PPVs occurred at dominant frequencies of greater than 250 Hz.

6.3 *Basement Wall response at building 2*

There is one basement location where there can be response without interaction with the surrounding soil and below-ground infrastructure: out of plane bending of the west basement wall adjacent to the excavation. Response of the basement mid-wall (W) transducer in Building 2 to the 08/05 blast demonstrates the extent to which the basement wall responds in this direction. This location is of particular interest as it is the only basement wall that 1) can respond freely without interaction with the surrounding soil and 2) is distorted directly by rock motions. Walls separating above-ground floors are excited by motions transmitted by the building, which decline significantly with distance from the blast location and elevation within the building.

Displacements of the mid wall (W) basement transducer at building 2 are employed to calculate tensile bending strains for shot h, and are compared to the others in Table 1. The out of plane, beam bending model is employed with time correlated displacements measured in the rock (G) and at the street level (B).The L distances needed for this calculation were those shown in Figure 2. As shown in Figure 7, three values of the relative transverse displacements, δ , can be calculated: either a) SBT-W, or b) W-GT components, or c) Wall- average (SBT-GT). Differential displacements between the transverse rock (GT) and mid-wall (W) motions are shown in Figure 8 (a) in relation to the velocity and displacement time histories.

The out of plane basement wall response is not large. The PPV of the mid-wall was 7.1 mm/s with a rock excitation of 5. 2 mm/s at 140 Hz. Calculated tensile bending strains of 0.8 to 2 μ-strains are similar to the tensile strains calculated from the in-plane shear strains in walls above the street level. They are small compared to the stains that are necessary to cosmetically crack brick mortar and weak wall covering (300 to 500 μ-strains) (Siskind2000).

6.4 *Comparison with previous studies of tall structure response in urban close-in blasting*

Strains measured in this study are lower than those observed in similar tall urban structures (Aimone-Martin, et al, 2014). Figure 9 compares data from this case with that of others by comparing calculated tensile strains with peak ground displacement up to 0.1 mm. Aimone-Martin data are presented as the insert to Figure 9, with both the figure and insert possessing the same range of shear strains (up to 7 μ-strains). While this study included situations with greater peak ground displacement, smaller strains were induced at the higher peak ground displacements and fall below the lower limit curve (A) and upper limit bound (B). The upper bound of all strains vs peak ground displacement is not exceeded.

6.5 *Measured strains are low despite the large magnitude of the peak particle velocity in the foundation rock.*

The potential for these measured strains to produce hair line, cosmetic cracks can be assessed by comparison with failure strains as reported by (Aimone-Martin, Meins, 2014) and summarized as follows. Visible surface cracks were observed in the weakest materials found in buildings at 300 μ-strains in drywall plaster core and aged mortar. Onset of visible mortar cracks between concrete masonry units appeared at 470 μ-strains (Siskind, 2000). No information is available in the U.S. literature on nonmilitary dynamic testing providing failure strains for lime and gypsum plasters typically used as wall coating in historic and older structures. Laboratory testing of typical Brazilian cement grout samples made with varying cement, lime, and water ratios and used for surface wall coating is reported by (Rosenhaim, et al (2014). Diametral and beam bending test results show failure strains range from 153 to 286 μ-strains. Therefore, a conservative threshold of 100 to 200 μ-strains can be employed as an indication of possible hairline cracking in historic plaster in the above ground portions of the structures.

7 SINGLE-DEGREE-OF-FREEDOM (SDOF) MODEL

7.1 *General Considerations*

Single Degree Of Freedom (SDOF) modeling of structural response is advantageous because it takes into account the time history of the excitation motion (dominant excitation frequency) as well as amplitude (PPV). Comparative SDOF modeling is instructive in this case since it returns relative displacement which is directly comparable with measured relative displacement. Since displacements are measured in the plane of the wall comparisons are made with excitation velocity time histories measured in a direction parallel to the response motions.

SDOF models consist of a mass, spring and dashpot, for which the relative displacement response of the spring can be calculated from the excitation motions at the base of the spring. The dynamic response properties of the structure can be defined by the natural frequency and percentage of critical damping. This model is described structural dynamics texts as well as in Dowding (2000). The model returns relative displacement for a given excitation motion, the maximum of which can be plotted as a pseudo velocity response for a range structural natural frequencies (F_n) and a common damping constant (5% in this case) as shown in Figure 4. Pseudo velocity is the relative displacement times the circular natural frequency of the structure, or $\delta*2\pi*F_n$.

Considerations of energy and mass show that response of large, urban structures to ultra-high frequency excitation is likely to be low. First consider single degree of freedom (SDOF) pseudo velocity response with 5% damping of the 06/02 event compared to shown with that from a large, distant quarry (Q) and close, tunnel (T) blast shown in Figure 4. Spectrum T was developed from ground motions recorded 12m (38ft) away from a 0 to 9 ms delayed tunnel blast with a maximum charge in any single delay of 1.7 kg (3.8lb). Spectrum Q was developed from the ground motions recorded 72m (220ft) away from a single 91 kg (200lb) charge detonated in a typical bench blast hole in a limestone quarry. The quarry blast generated a peak radial particle velocity of 43 mm/s (1.7 in/s) and the tunnel blast generated a peak radial particle velocity of 61 mm/s (2.39 in/s) (Dowding, 2000). The 06/02blast generated a radial peak particle velocity of 51 mm/s in the rock from a 2.4 kg blast some 9+ m distant from building 1.

Even though the peak particle velocities are similar, standard pseudo-velocity response spectrum analysis in Figure 4 predicts that a single story, 10Hz structure or component will sustain pseudo response velocities that are 50 and 5 times larger for the quarry and tunnel blasts than for the 06/02 ultra-high frequency event. Since the pseudo velocity is proportional to relative displacement for structures with the same natural frequency (10 Hz in this discussion), the 06/02 event would be expected to induce far less relative displacement, strain, and cosmetic cracking than induced in a typical single story residential structure or 10 Hz component.

7.2 *Use of SDOF as Control Index*

It is instructive to compare measured relative displacement (or strain) with indices for control of the potential for cosmetic cracking to determine their effectiveness. The most often employed index is peak particle velocity (PPV) ground motion which is measured immediately adjacent to the structure in the ground. In urban construction PPVs are measured often on the structure at the street level or in the basement of the structures because of the lack of ground between excavation and the structure.

Single degree of freedom (SDOF) response can also be employed as an index of cosmetic cracking using ground motion time histories. It is a more robust index than the PPV because it includes, as described above, the effects of the frequency of excitation relative to the natural or fundamental frequency of the structure of concern. SDOF systems can be employed for both single and multiple story structures. Calculations (Dowding, 2000) have shown that the ratio of pseudo velocity response divided by the excitation peak particle velocity calculated with a SDOF system is within 15% of the same ratio when calculated with a three floor or three degree of freedom system (Dowding, 2000). These calculations were made with excitation motions that were at the 2^{nd} and 3^{rd} mode frequencies (2.8 and 4.5 times the fundamental frequency). The SDOF response index is employed herein only as an index of the severity of imposed strains.

As shown in Appendix A relative displacements and strains induced in urban structures by ultra-high blast induced rock motions are very small; 30 μm in the basement and 3 μ strains in the super structure for 50 mm/s PPV excitation. Their minimal magnitude is further illustrated in Table 1 by comparing urban structure responses with those of a variety of residential structures to surface coal mining blasts (Dowding & McKenna, 2005). Measured (structure-ground) differential displacement (column 3, third column from the left) is compared to the SDOF values (column 4) calculated from the ground motions. Responses of the 4+ story urban structure of this study (Building 1) are tabulated in the upper half of the table and those of four single story residential structures are tabulated on the lower half. Measured displacements are those from time correlated differences of integrated velocities, and SDOF calculations were made from the ground or rock excitation motion with 5% damping. SDOF calculations were made for a range of response frequencies that included both the natural frequency of the superstructure (10 residential and 2.5 Hz urban) and those of walls and attachments (15 residential and 16 Hz urban).

Comparisons in Table 1 allow several observations to be made. As illustrated with the response spectra in Figure 4, ultra-high frequency excitation should produce significantly lower responses than lower frequency excitation with similar PPV's. Table 1 verifies this observation with the exception of shot d, which will be discussed below. Measured relative displacement in column 3 of the urban structure with an excitation PPV of 27 mm/s is 20 μm while for a residential structure with an excitation PPV of only 8 mm/s it is 250 μm. The ratio of (residential strain to urban strains) per (residential PPV to urban PPV) is some (200/20)/(8/27) = >34. Measured relative displacements also match those calculated from SDOF response with ground motion time histories for both the high (urban) and low (residential) frequency excitation ground motions.

Estimating expected relative displacements for high frequency response of urban structures on the basis of PPVs yields estimates that are opposite to that measured. If relative displacement is a function of PPV only, and experience with residential structures indicates relative displacements of 200 μm are produced by PPVs of 6 mm/s then shots b and d should have produced relative displacements of 200*(130 to 200)/6 = 5300 μm. Measured relative displacements produced by excitation with PPVs of 25 mm/s at ultra-high frequencies are only 20 μm, which is less than 1/100th of that expected from experience with low frequency excitation of residential structures, if PPV is employed at the index. Calculated response (based on SDOF calculation) more closely matches that measured.

A comment about shot d and its SDOF calculation is necessary as it is unusual. The measured relative displacement between the rock and first floor was similar to that calculated with the SDOF response. As shown by the time histories in Appendix B shot d's high PPV was produced by a single velocity pulse at 500 Hz which was incapable of displacing the first floor by more than $1/10^{th}$ that of the excitation displacement because of its low impulsive energy. Even with a PPV of some 200 mm/s shot d produced relatively small strains of some 60 μ strains in the basement and only 6 μ strain in the superstructure as shown in Table 1. This absorption of energy is discussed above and in greater detail elsewhere (Hamdi, 2015)

The deminimus magnitude of the measured relative displacements and strains of urban structures in Table 1 and Appendix A is further verified in Table 1 by crack response data of residential structures on the right side. The last two columns on the right side of Table 1 compare response of cosmetic cracks in residential structures to climatological (last column) and blast vibration (next to last column) (Dowding and McKenna, 2005). Both vibratory and climatological (temperature and humidity) responses are measured by the same micrometer displacement transducer at the same crack location. Comparison of the two right most columns shows that climatological effects (far right column) produced 5 to 20 times more response of cosmetic cracks than the blast induced vibratory distortion. This relatively low level of cosmetic crack response in the residential structures occurred with blast induced relative displacements (distortions) of 130 to 250 μ m. (third column from the left). Despite PPV's that exceeded 50 mm/s the urban structures sustained lower relative displacements and strains (columns 3 and 5) than did the residential structures with PPV's of 3-8 mm/s, which are in turn 5 to 20 times smaller than climatological crack response.

8 COMPARISON WITH USBM SAFE BLASITNG CRITERIA FOR RESIDENTIAL STRUCUTRES

Impact of ultra-high frequency excitation ground motions can be assessed by comparing them to the USBM "Z" curve criteria (Siskind, et al, 1980) modified (Aimone-Martin at al, 2014) and European, DIN standards (DIN, 1999). Time histories of the motions of the eight events were converted to a PPVs- dominant frequency format and plotted with the Z curve in Figure 10. The second plateau (from the left) in Figure 10 represents a typical 100 mm/s control limit for blasting adjacent to urban structures with line drilled holes to separate the fragmented volume from the rock beneath the adjacent structure. Rock ground motions (solid dots) are identified by letters defining blasts located in Figure 1 and tabulated in Appendix A. Dominant frequency was determined by calculating the zero crossing times for the pulse with the greatest amplitude. Particle velocities measured at street level (NB & SB) are also plotted as these are often assumed to be the default motions because of the inaccessibility of the rock surface.

Even though rock motions for shots b,c and d plot above the 100 mm/s control line for frequencies above 200 Hz, the measured relative displacements and strains were small as shown in Appendix A and Table 1. Generally speaking, the rock motion (circles) displays the highest frequencies and highest PPVs. Motions at the street level north (triangles) whose frequencies ranged from 36 Hz to 250Hz fall below the extended "Z" curve control limits.

This comparison of excitation motions with and extended "Z" curve control limit demonstrate the usefulness of additional measurement of structural response. Even though the rock excitation motions exceeded the 100 mm/s bound above 100 Hz, they induced low relative displacements and strains in the structure. Thus it has been suggested (Aimone et al, 2014) that measurement of building response at multiple, structurally significant locations can serve as the (or a supplemental) mechanism for regulatory control of urban blasting vibrations.

8 CONCLUSIONS

Time correlated velocity response to ultra-high frequency blast vibration excitation was measured at multiple positions in two urban buildings. These measurements and their analysis allow the following observations regarding blast induced strains. These observations are based upon tangential and radial velocity responses at ten positions during eight blast events, which provided over 70 time histories for analysis. Strains in these multiple story, urban structures are compared to those measured in one to two story, residential structures, whose response serves as the basis of many current blasting regulations.

- Close-in blasting practice with line-drilling combine to produce ultra-high frequency excitation pulses with short duration.
- Despite high peak particle excitation velocities, differential displacements (and thus strains) along a structure are similar to and often less than those measured in residential structures excited by lower than regulation limited peak particle velocities.

- Strains measured on these urban structures produced by ultra-high frequency, high peak particle velocities are lower than those necessary to crack masonry structures and weak wall covering materials.
- Measurement techniques presented herein demonstrate how strain calculated from differential displacement can be employed to control blasting activities.
- Relative displacement response calculated with damped single degree of freedom models of the structures generally matches that measured when excitation motions are those measured in the rock for basement response and at the street level for superstructure response.

ACKNOWLEGEMENTS

This paper is the result of an unusual set of fortuitous circumstances and the authors wish to acknowledge the organizations and special circumstances that allowed the writing of the paper. First, the New York City Fire Department for their interest in allowing this activity to further the science of blast vibration monitoring. Second, building owners and their contractors, for their cooperation and coordination given the inevitable intrusions necessary to instrument structures in the midst of complicated and compact construction foot print. Third the members of the Aimone-Martin Associates, especially Brent Meins, for installing and maintaining the operability of the instruments during the course of the investigation. Fourth, the GGGE Program of the CMMI Division of the National Science Foundation who provided the additional funds to time correlate the instruments through the RAPID Response initiative. Finally, the U.S. Embassy in Tunis, as well as the U.S. Department of State, Bureau of Educational and Cultural Affairs and the Council for the International Exchange of Scholars for their assistance and support during the Fulbright Visiting Research Fellowship of Dr Essaieb Hamdi at the Civil and Environmental Engineering Department of the Northwestern University.

References

Abeel P.A. (2012) Building and Crack Response to Blasting, Construction Vibrations and Weather Effects. Northwestern University Master of Science thesis. 114p

Aimone-Martin C., Meins B., Lauer J., Brent R (2014). Tall structure response to close-in urban blasting in New York City. The Journal of Explosives Engineers, 16p.

Aimone-Martin, C.T., Meins, B.M., (2014) Tall Structure Response to Close-in Blasting in New York City – A Comparison with Residential Structure Response, 40th Annual Conference on Explosives and Blasting Techniques, International Society of Explosives Engineers., Cleveland, OH, USA

DIN 4150, 1999. Part 3, Structural vibration - Effects of vibration on structures

Dowding, C.H. (2000) Construction Vibrations, Available through Amazon. 1996 version: Prentice Hall, NJ, USA, 620 pa

Dowding, C.H. and McKenna (2005) Crack Response to Long-Term Environmental and Blast Vibrations Effects, ASCE Journal of Geotechnical and Geoenvironmental Engineering, Vol. 131, No. 9, Sept pp 1151-1161.

Hamdi E. (2015) Analysis of urban buildings response to close-in blasting induced vibrations. Fulbright Visi ting Research Scholar Program report. Department of Civil and Environmental Engineering, Northwestern University, Evanston, IL 79 pages.

Oriard, L. L. (1972) "Blasting Effects and Their Control in Open Pit Mine" *Proceedings of Second International Conference on Stability in Open Pit Mining,* C.O. Brawner and V. Milligan, editors, ASME-AIME, Littleton, CO,pp 197-222.

Panish, P.T. (1992) The Mt. Prospect region of western Connecticut; mafic plutonism in Iapetus-sequence strata and thrust emplacement onto the North American margin, IN Robinson, Peter, and Brady, J.B., eds., Guidebook for field trips in the Connecticut Valley region of Massachusetts and adjacent states; Volume 2: University of Massachusetts, Geology Department Contribution, no. 66, New England Intercollegiate Geological Conference, 84th Annual Meeting, Amherst, MA, October, 9-11, 1992, p. 398-423.

Rosenhaim, V.L., Aimone-Martin, C.T. Munaretti, E., Koppe, J.C. (2014) Structure and Crack Response to Coal And Quarry Blasting In Brazil, 40th Annual Conference on Explosives and Blasting Techniques, International Society of Explosives Engineers, Cleveland, OH, USA

Siskind, D.E. (2000) Vibrations from Blasting, International Society of Explosive Engineers, Cleveland Ohio, USA, 120 pgs

Siskind, D.E., M. S. Stagg, J. W. Kopp, and C. H. Dowding, (1980) Structure Response and Damage Produced by Ground Vibration from Surface Mine Blasting, U.S. Bureau of Mines, RI 8507.

Woods, R. & Jedele, J. (1985) "Energy-Attenuation Relationships from Construction Vibrations," in *Vibration Problems in Geotechnical Engineering* (G Gazetas and E.T. Selig, Eds.), Special Technical Publication, ASCE, New York, pp. 187-202.

.

Appendix A

Table A. Strain level estimation in the different parts of the two investigated buildings.

Building	Set	Blast	Shot	Transd	PPV (mm/s)	frq (Hz)	PPV/frq (~mm)	Position	Diff (μm)	S Strain (μ-strains)		T Strain (μ-strains)
				NBR	10.3	111	0.093	NR(A-B)	54.8	4.7		0.9
				NBT	10.8	91	0.119	NT(A-B)	37.4	1.3		1.3
				NAR	6.6	91						
				NAT	6.1	36						
		06/30	e	SBR	2.5	200	0.013	SR(A-B)	7.9	0.3		0.1
				SBT	1.5	111	0.014	ST(A-B)	7.9	0.3		0.1
				SAR	1.5	34						
				SAT	0.9	16						
				NBR	24.4	125	0.195	NR(A-B)	132.8	11.0		2.1
				NBT	17.3	63	0.275	NT(A-B)	136.5	12.0		4.8
				NAR	16.8	63						
		06/27	f	NAT	19.8	63						
				SBR	5.2	59	0.088	SR(A-B)	14.6	0.5		0.2
				SBT	2.9	100	0.029	ST(A-B)	14.7	0.5		0.3
				SAR	2.5	34						
				SAT	1.7	17						
				NBR	19.3	167	0.116	NR(A-B)	178.7	15.0		2.8
				NBT	22.9	77	0.297	NT(A-B)	113.9	9.8		4.0
				NAR	21.3	77						
	Set 1	07/07	g	NAT	8.5	67						
				SBR	2.4	125	0.019	SR(A-B)	12.1	0.4		0.2
				SBT	1.7	36	0.047	ST(A-B)	10.5	0.4		0.2
				SAR	2	36						
				SAT	1.1	18						
				NBR	7.6	125	0.061	NR(A-B)	17.8	1.5		0.3
				NBT	6.6	77	0.086	NT(A-B)	21.6	1.9		0.8
				NAR	3.6	59						
				NAT	4.1	63						
1		08/05	h	SBR	4.7	111	0.042	SR(A-B)	8.1	0.3		0.1
				SBT	1.1	100	0.011	ST(A-B)	12.1	0.4		0.2
				SAR	1	42						
				SAT	1.1	15						
				NBR	12.8	77	0.166	NR(A-B)	62.3	5.4		1.0
				NBT	13.6	125	0.109	NT(A-B)	54.4	4.7		1.9
				NAR	6.1	71						
		06/05	b	NAT	8	29						
				GR	39.4	333	0.118	GR(B-G)	33.1	5.7		2.8
	Set 2			GT	128.8	500	0.258	GT(B-G)	89.1	15.3		6.3
				NBR	15.7	77	0.204	NR(A-B)	49.7	4.3		0.8
				NBT	9.8	167	0.059	NT(A-B)	69.8	6.0		2.5
		06/09	d	NAR	7.1	71						
				NAT	10.3	59						
				GR	201.4	500	0.403	GR(B-G)	208.7	36.0		0.6
				GT	200.4	500	0.401	GT(B-G)	334.4	57.7		1.3
				NBR	6.6	100	0.066	NR(A-B)	32.9	2.8		0.5
				NBT	5.1	59	0.086	NT(A-B)	27.9	2.4		1.0
				NAR	7.1	100						
				NAT	4.4	53						
		06/02	a	SBR	9.1	200	0.046	SR(A-B)	19.6	0.7		0.3
				SBT	3.8	200	0.019	ST(A-B)	12.6	0.7		0.4
				SAR	1.5	42						
				SAT	1.7	17						
				GR	51.6	500	0.103	GR(B-G)	33.8	5.8		0.1
				GT	27.4	333	0.082	GT(B-G)	19.3	3.3		0.2
	Set 3			NBR	12.1	83	0.146	NR(A-B)	63.1	5.4		1.0
				NBT	10.8	143	0.076	NT(A-B)	58.0	5.0		2.1
				NAR	6.6	45						
				NAT	10.2	71						
				SBR	4.1	250	0.016	SR(A-B)	11.2	0.4		0.2
		06/06	c	SBT	2.4	100	0.024	ST(A-B)	15.1	0.6		0.3
				SAR	2	31						
				SAT	1	15						
				GR	131.6	500	0.263	GR(B-G)	127.1	21.9		0.2
				GT	70.4	250	0.282	GT(B-G)	72.9	12.5		0.8
				SBR	3	83	0.036	SR(A-B)	17.8	1.1		0.5
				SBT	4.1	100	0.041	ST(A-B)	18.7	1.2		0.5
				SBT	4.1	100	0.041	WT(B-W)	19.1		2.0*	2.0
2		08/05	h	SAR	4.1	83						
				GT	5.2	143	0.036	GT(B-G)	17.4	3.0		1.4
				GR	19.4	500	0.039	GR(B-G)	17.4	3.0		0.6
				SAT	2	71						
				GR	19.4	500						
				GT	5.2	143	0.036	WT(G-W)	18.4		0.8*	0.8
				GT	5.2	143	0.036	WT(W-Avg(SBT,GT))	17.5		1.9*	1.9
				W	7.1	50						

* Bending strains

Distances used for the strain computation:

- H=11.6m and W=22.2m for the North transverse components and H=11.6m and W=61m for the north radial components for the Building 1;
- H=27.4m and W=22.2m for the South transverse components and H=27.4 and W=61m for the south radial components for the Building 1.
- H=5.8m and W=22.2m for the North rock to bottom transverse components and H=5.8m and W=61m for the north rock to bottom radial components for the Building 1.
- H=15.8m and W=7.6m for the transverse components and H=15.8m and W=26.2m for the radial components for the Building 2;
- H=3.5m and W=7.6m for the rock to mid-wall transverse components and H=3.5m and W=26.2m for the rock to mid-wall radial components for the Building 2;
- H=2.2m and W=7.6m for the mid-wall to bottom transverse components and H=2.2m and W=26.2m for the mid-wall to bottom radial components for the Building 2.

Appendix B

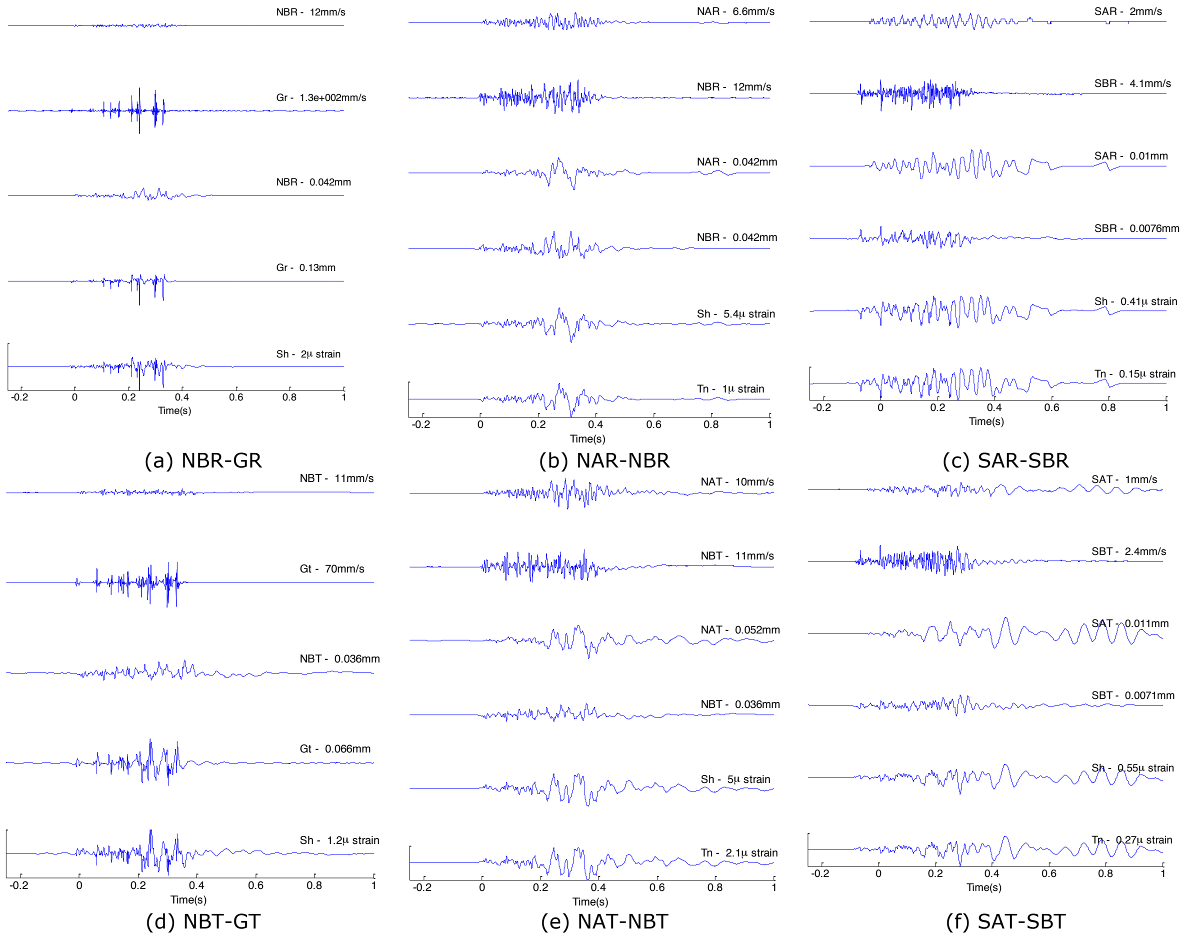

Figure B.1. Strain level calculations for blast 06/06.

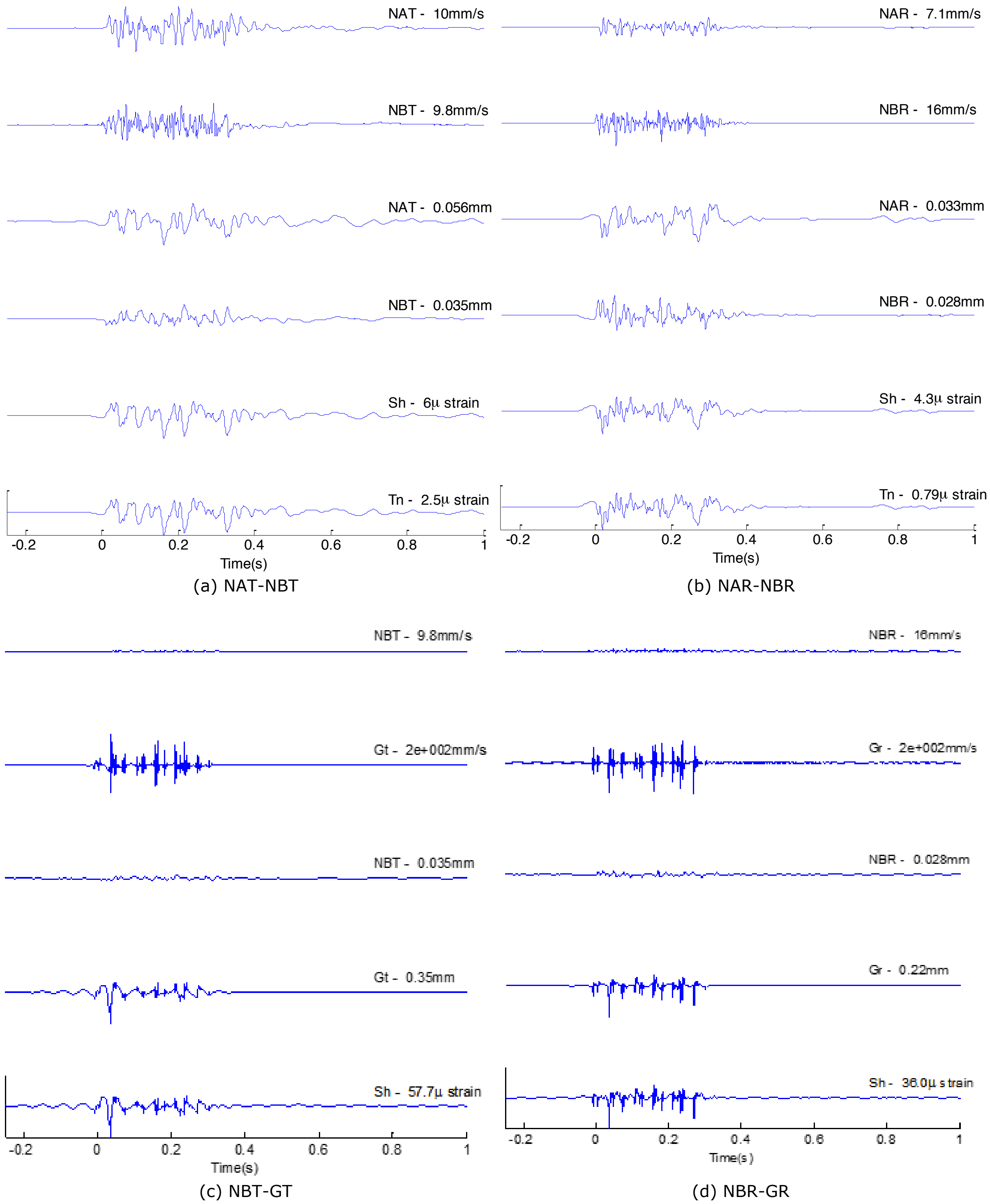

Figure B.2. Strain level calculations for blast 06/09.

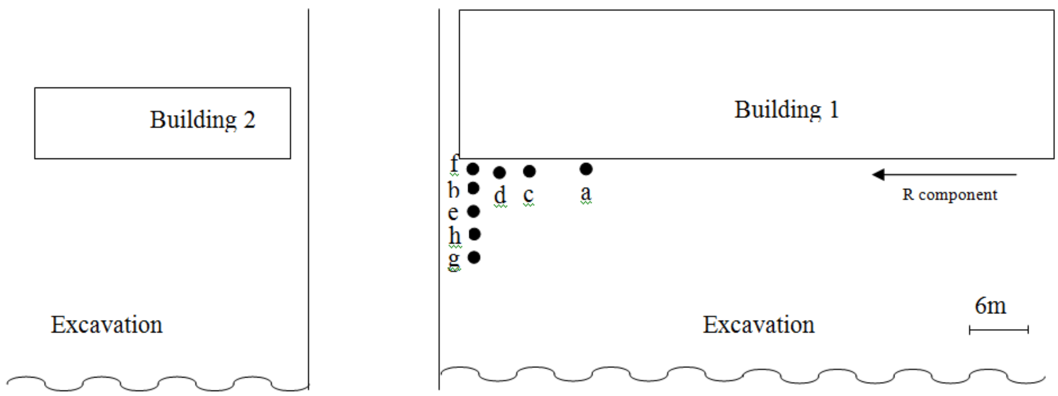

Figure 1. Blast locations with regards to the buildings. The close proximity and simultaneous construction allows blast response from ground motions with high amplitudes and ultra-high frequency to be measured at both buildings. (a: blast 06/02/2014; b: blast 06/05/2014; c: blast 06/06/2014; d: blast 06/09/2014; e: blast 06/27/2014; f: blast 06/30/2014; g: blast 07/07/2014; h: blast 08/05/2014).

Foundation details of Building 1 *Foundation details of south end of Building 2*

Figure 2. Locations of the sensors at the upper and lower parts of the monitored walls at the two buildings.

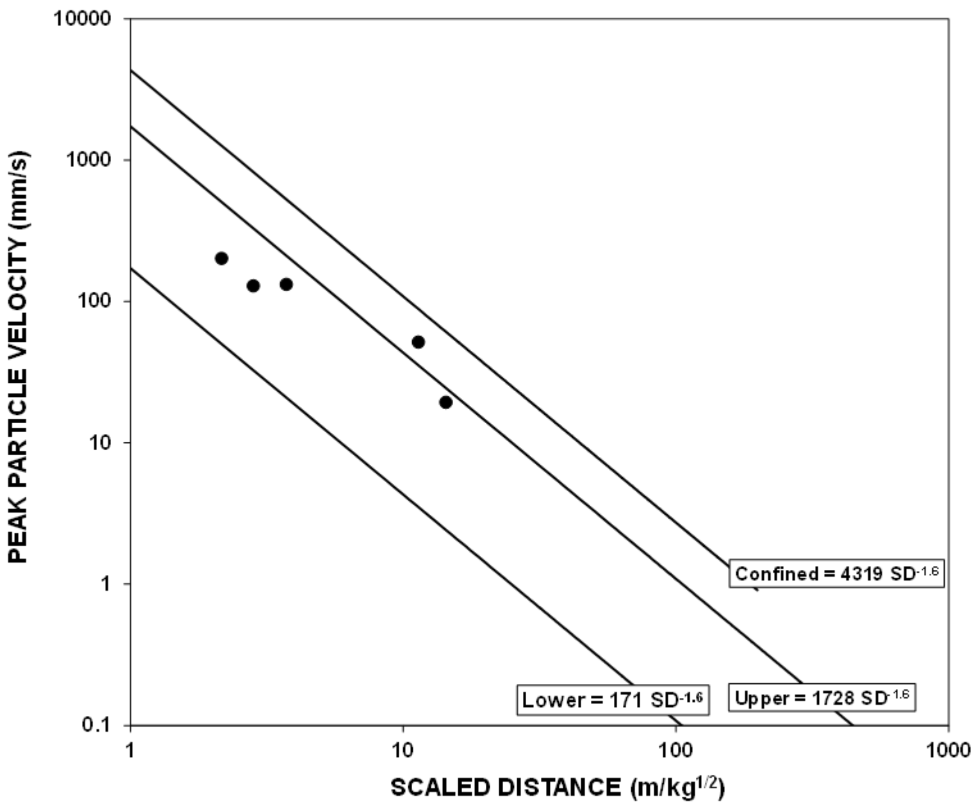

Figure 3. Comparison of measured square root scaled distance attenuation and Oriard's (1972) expected values for typical practice showing the difference between rock to rock transmission (rock data) and rock to street (NB data). Curve C is for confined conditions and B and A are upper and lower bound of expected values.

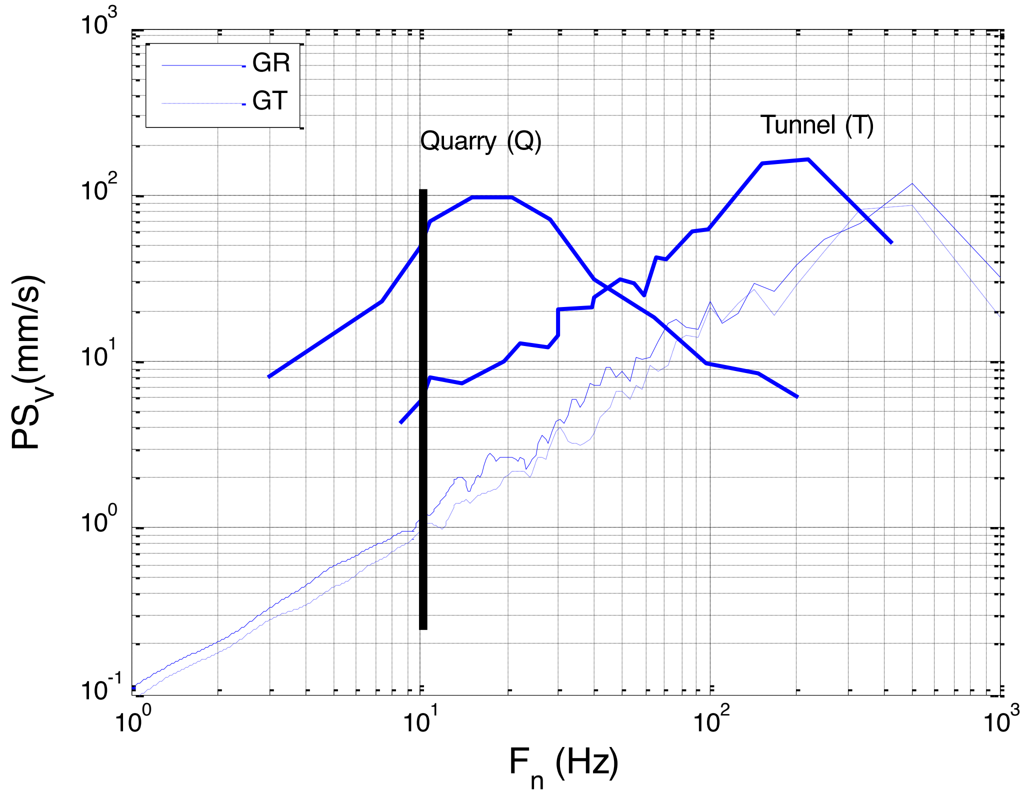

Figure 4. Comparison of response spectra of ground motions from close-in blast event 06/02 and a low frequency quarry blast (Q) and a near-by tunnel blast (T); GR (solid line and generally larger) and GT are rock motions in N-S and E-W directions respectively.

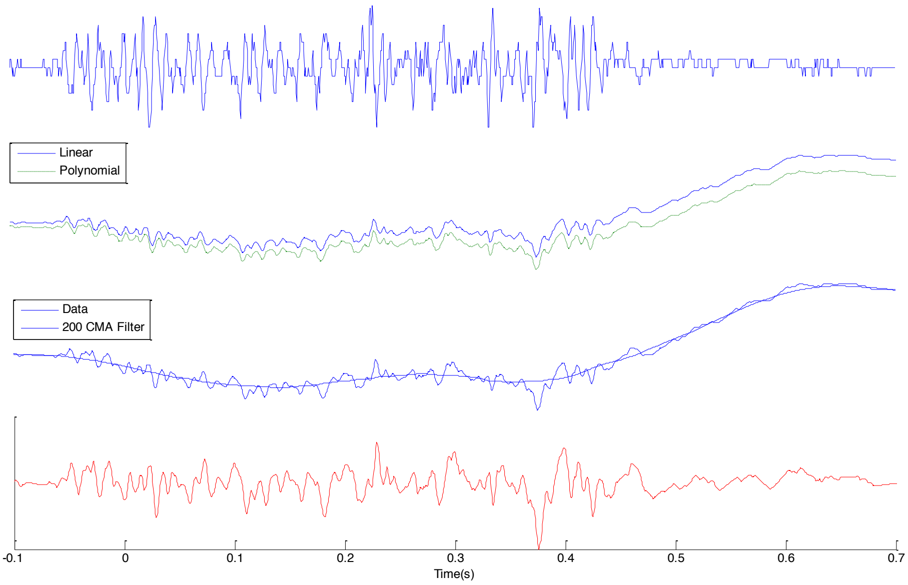

Figure 5. Displacements calculation using baseline correction and 200 point central-moving-average filtering (case of SBT recording at Building 2): (a) (top) Velocity recording, (b) Displacement after linear (solid and generally higher) and second order polynomial baseline correction, (c) 200 point central-moving-average fit to the second order baseline corrected displacement data, (d) (bottom) Final displacement obtained by subtracting the 200 CMA from the data.

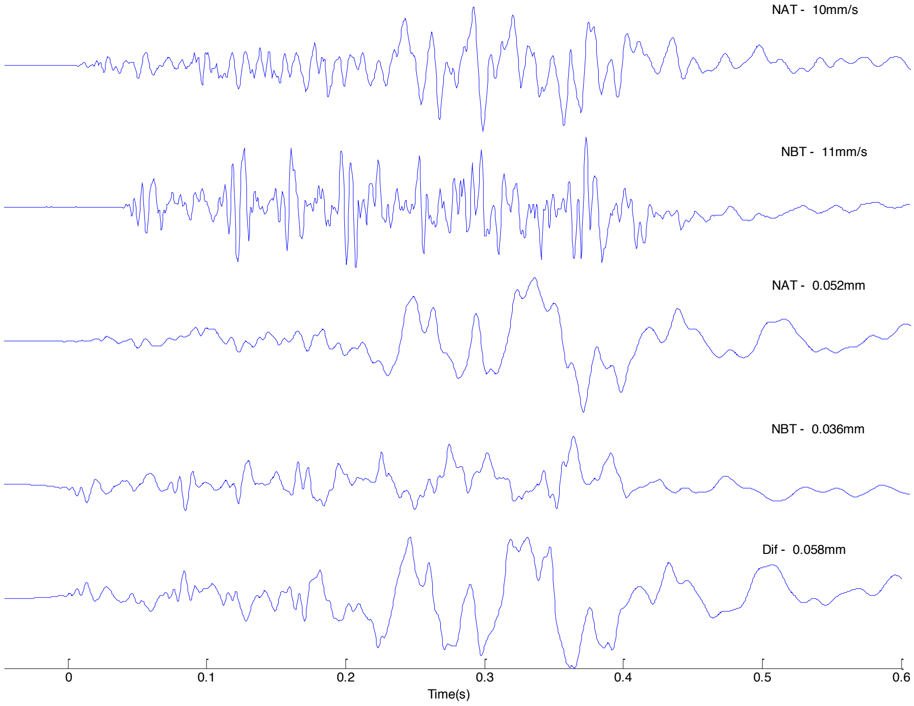

Figure 6. Example calculation of the difference in transverse displacements between the top and bottom of the north corner of building 1 for the 06/06 event: a) top two time histories–velocities at top (NAT) and bottom (NBT); b) middle two time histories – displacements at top and bottom and c) bottom time history – difference between top and bottom displacements. Velocities and displacements are plotted at consistent scales, where the amplitudes given at the right are those of the peaks.

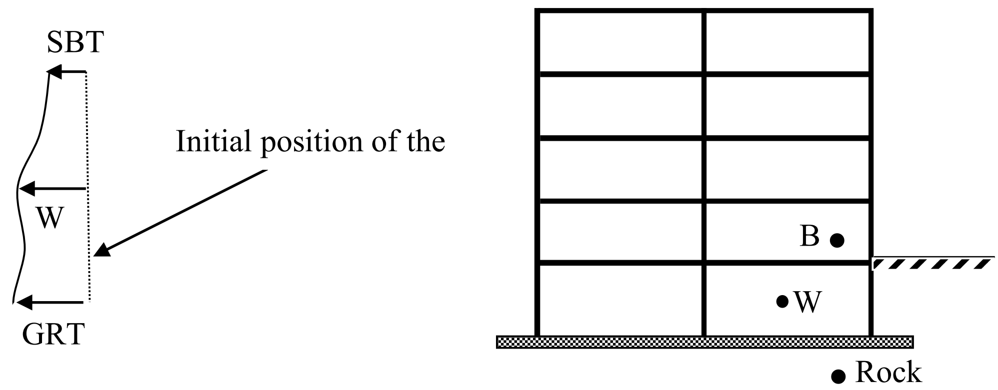

Figure 7. Displacement in the bottom southern part of the wall in Building 2 (W: Mid-wall, SBT: south lower, GRT: transverse ground motion).

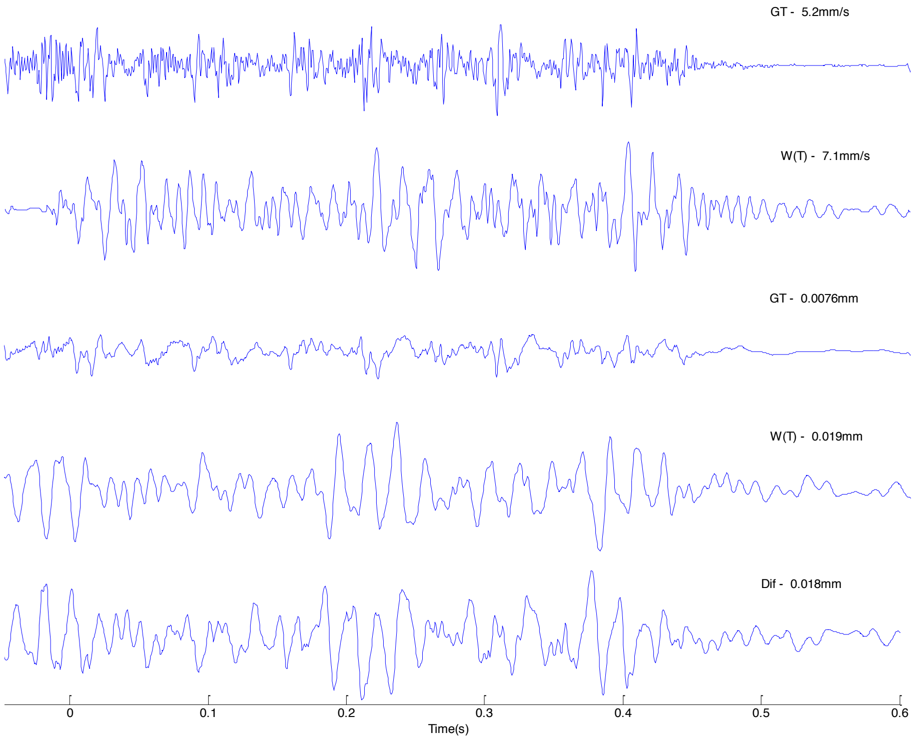

Figure 8. Differential displacements calculation using baseline correction and 200 point central-moving-average filtering (case of rock and mid-wall recordings at Building 2 during blast 08/05/2014): (a) and (b) Velocity recordings, (c) and (d) Displacements after second order polynomial baseline correction, (e) Final differential displacement. Velocities and displacements are plotted at consistent scales, where the amplitudes given at the right are those of the peaks.

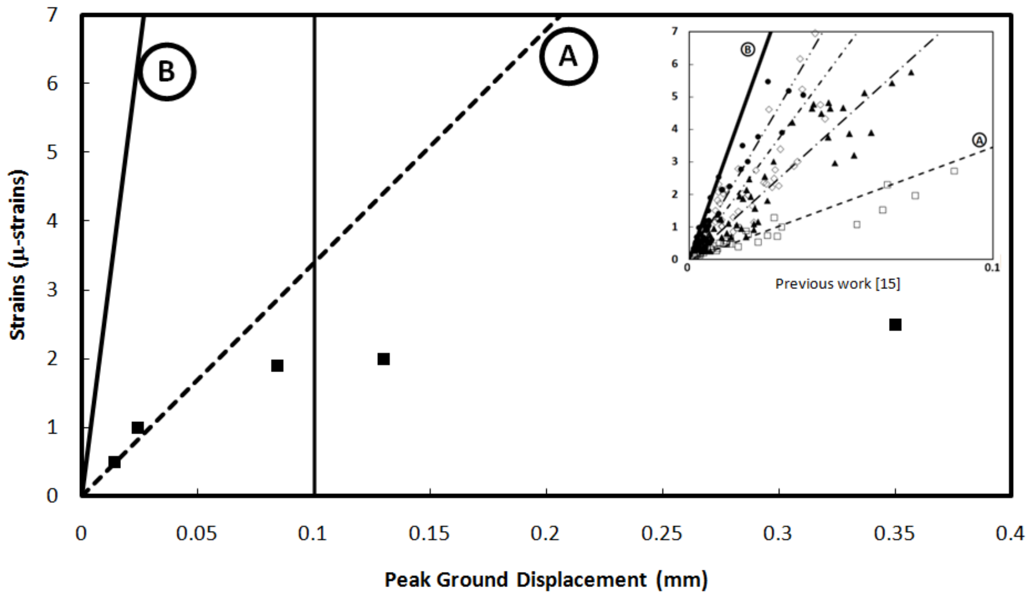

Figure 9. In plane tensile strains at the top and bottom of buildings versus peak ground displacement. Comparison with Aimone et al (2014)

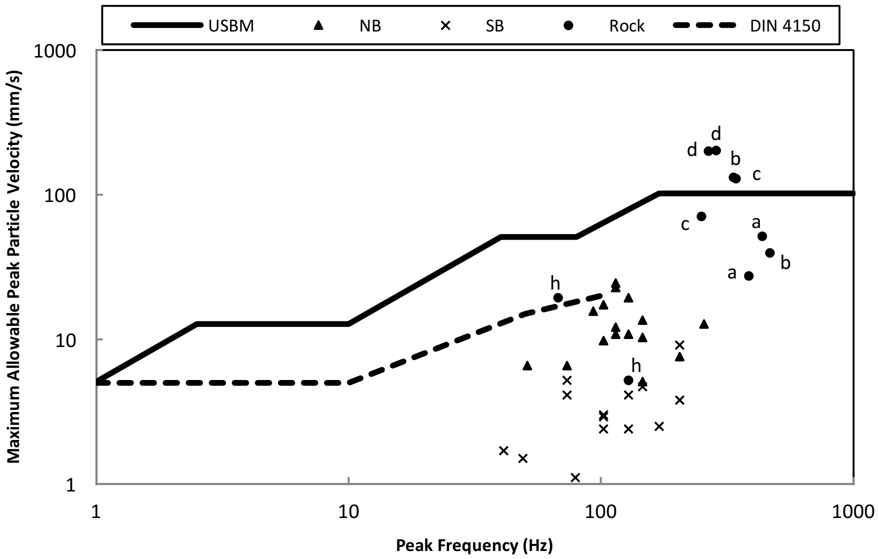

Figure 10. Frequency and Maximum Peak Velocity compared to the safety USBM and DIN 4150 criteria. Extension of the USBM control above 100Hz has been suggested to use with close-in blasting (Aimone et al 2014).

Table 1

Measured and SDOF Calculated Responses of Structures to Low and Ultra-High Frequency Blast Excitation

	Basement and One Story Response					Above Ground Response					Crack Response	
	PPV Rock	Freq Excite	Relative Displacement Measured	Relative Displacement Calculated Rock	Shear Strain Measured	PPV Grd Floor	Freq Excite	Relative Displacement Measured	Relative Displacement Calculated Street	Shear Strain Measured	Peak Vibration	Max Weather
	mm/s	HZ	µm	µm	µ strain	mm/s	HZ	µm	µm	µ strain	µm	µm
4 to 5 Story Urban Building (1)				2.5-16 Hz	h = 5.8m				2.5-16 Hz	h = 11.6 m		
Shot a	27.4	333	20	14-16	3.3	5.1	59	28	22-27	2.4		
Shot c	70.4	250	72	59-121	12.5	10.8	143	58	31-51	5		
Shot b	132.6	500	89	74-87	15.1	13.6	125	54	36-48	4.7		
Shot d	198.1	500	334	360-471	57.5	9.8	167	70	32-92	6		
4 to 5 Story Urban Building (2)												
Shot h (basement midwall response)	5.1	143	18		2[1]							
Single Story Residential Structures				10-15 Hz	h = 2.5m							
Trailer: Pennsylvania	3.6	7 to 20	210	240-180	86.1						4.2	24
Bungalow 1: Indiana	5.8	6 to 25	180	170-95	73.8						0.3	12
Wood Frame: Indiana	7.6	15 to 20	133	150-259	54.5						13.6	52
Adobe: New Mexico	8.1	4 to 14	250	230-80	102						0.9	25

1 Bending strain